Revisiting the fragile-to-strong crossover in metallic glass-forming liquids: Application to Cu$_x$Zr$_x$Al$_{100-2x}$ alloy

René Alvarez-Donado[*] and Samuel Cajahuaringa[†]

Instituto de Física Gleb Wataghin, Universidade Estadual de Campinas, UNICAMP, 13083-859 Campinas, São Paulo, Brazil

Alex Antonelli [●][‡]

Instituto de Física Gleb Wataghin and Center for Computing in Engineering & Sciences, Universidade Estadual de Campinas, UNICAMP, 13083-859 Campinas, São Paulo, Brazil

The fragile-to-strong crossover seems to be a general feature of metallic glass-forming liquids. Here, we study the behavior of shear viscosity, diffusion coefficient, and vibrational density of states for Cu$_x$Zr$_x$Al$_{100-2x}$ alloy through molecular dynamics simulations. The results reveal that the fragile-to-strong temperature (T_{fs}) and the glass transition temperature (T_g) increase as the aluminum content becomes larger. The inverse of the diffusion coefficient as a function of temperature exhibits a dynamical crossover in the vicinity of T_g, at a much lower temperature than that predicted by nearly all previous studies. At the temperature in which the dynamical crossover occurs determined by the inverse of the diffusion coefficient, we found an excess of vibrational states at low frequencies, resembling a pronounced peak in the reduced vibrational density of states characteristic of a strong liquid. Finally, the behavior of the shear viscosity as a function of reduced temperature (T_g/T) also shows that, aside from the fragile-to-strong crossover nearby T_g, another dynamical crossover is present near the onset of the supercooled regime.

I. INTRODUCTION

Almost 60 years after having synthesized the first metallic glass [1], the nature of such materials, as well as other glasses, remains an unsolved problem in condensed matter physics and materials science [2,3]. In particular, the temperature at which a liquid becomes a glass, the glass transition T_g, is strongly dependent on the chemical composition and the cooling rate used to obtain the glass [4,5]. Therefore, it is not possible to set a single value for T_g, and different criteria are used to define when a liquid becomes a glass. A common criterion is to choose T_g as the value at which the shear viscosity of the liquid attains a value of 10^{13} poise.

Angell [6] proposed a classification of glasses according to the thermal behavior of the shear viscosity, thus defining the concept of liquid fragility. Glass-forming liquids are called strong when their shear viscosity is reasonably well described by a single Arrhenius equation, presenting a low fragility index. On the other hand, liquids that cannot be described by a single Arrhenius equation are called fragile, and present a high fragility index compared to strong liquids [3]. For most nonmetallic glass-forming liquids a single fragility index describes the full range of temperatures. Nevertheless, some liquids in the supercooled regime, such as water [7,8], silica [9,10], BeF$_2$ [11], specific compositions of

yttria-alumina [12], and triphenyl-phosphite [13], do not fit into either of the two categories. Since they present two fragility indices, for low and high temperatures, such liquids exhibit a dynamical crossover, starting as a fragile liquid and transforming into a strong liquid in the vicinity of T_g. On the other hand, this fragile-to-strong crossover (FSC) seems to be a general feature of metallic glass-forming liquids (MGFLs) [14,15].

In order to understand the reason for this crossover in the supercooled regime several theories have been proposed. A study explaining the glass transition through elastic waves in liquids [16] predicts the FSC in the supercooled regime in the vicinity of T_g as a consequence of local relaxation events in all systems leading to a temperature-independent activation energy. Another attempt at describing FSC is based on the extended mode coupling theory (MCT) [17]. In such theory, the diffusion coefficient and the relaxation time change their behavior from non-Arrhenius to Arrhenius at a temperature value approximate to the critical temperature T_c of the original version of MCT. Computational and experimental works have been carried out in parallel to uncover the nature of FSC. Chen *et al.* [8] found a FSC in supercooled water by studying the thermal behavior of the inverse of the self-diffusion coefficient and the average of translational relaxation time. Zhou *et al.* [15] proposed the approximate relation $T_{fs} \approx 1.36T_g$, based on experimental data for 98 glass-forming liquids. FSC was found experimentally in Zr-based [15,18] and more recently in Fe-based [19] MGFLs. Moreover, in spite of various theoretical and experimental approaches already utilized in order to understand the reason behind the FSC, its origin remains unclear.

———————
[*]ralvarez@ifi.unicamp.br
[†]samuelif@ifi.unicamp.br
[‡]aantone@ifi.unicamp.br

Currently, two dynamical crossovers emerge when MGFLs are quenched to form a glass. The first happens near the onset of the supercooled regime and is associated with a transition from an uncorrelated liquid dynamics to a state of increasing cooperation in various regions [20,21]. During this transition, the transport properties deviate from Arrhenius to non-Arrhenius behavior. The second crossover is the fragile-to-strong one, which occurs in the vicinity of T_g. In this work, we present evidence from computer simulations of FSC for three $Cu_xZr_xAl_{100-2x}$ MGFLs. We choose this type of alloys because it is an ideal model, widely used to explore the properties of metallic glasses [15,18,22–27]. It is known that a small percentage of aluminum increases the fragility index and the glass transition temperature, allowing the exploration of changes in dynamical properties using molecular dynamics simulations [28]. The FSC in Cu-Zr-Al alloys has been verified in experimental studies and suggested by simulation analysis [15,22,23]. Notwithstanding, the previous experimental studies are based on values of viscosity obtained at high temperatures when the first dynamical crossover has not happened yet, and, therefore, the value of T_{fs} could be overestimated. To the best of our knowledge, we are not aware of any computational study that confirms the existence of the FSC in Cu-Zr-Al MGFLs by showing directly the change in the behavior from non-Arrhenius to Arrhenius in either the diffusion coefficient or the shear viscosity. In view of that, we conducted further investigations into the evidence of FSC in metallic glasses through computer simulations. For this purpose, we analyzed the temperature dependence of diffusion coefficient, vibrational density of states, and shear viscosity of CuZr(Al) MGFLs using an embedded atom method (EAM) potential developed by Cheng *et al.* [29], which adequately describes the properties of Cu-Zr-Al interatomic forces.

The remainder of the paper is organized as follows: Section II describes the methods used in this study for the calculation of the thermodynamic and dynamic properties of the alloys; results and discussion are presented in Sec. III; and, finally, Sec. IV conveys our conclusion.

II. METHODS

A. Simulation setup

The computer simulations were carried out employing the widely used molecular dynamics (MD) open code LAMMPS [30]. At first, we started with a binary alloy Cu-Zr, constituted by 4000 atoms (2000 Cu atoms and 2000 Zr atoms) in a cubic box subject to periodic boundary conditions in all three dimensions. An embedded-atom method (EAM) potential was used to describe the interatomic interactions [29,31]. Once the liquid at 2000 K reached the equilibrium, the alloy was quenched to 300 K at a rate of 100 K/ns. The quench was performed in the isobaric-isothermal (NPT) ensemble at zero external pressure. The Nosé-Hoover equations were integrated using a time step of 2 fs, with the pressure and temperature damping parameters of 200 fs and 5 ps, respectively. During the quenching process, several configurations were saved in order to obtain the dynamic and thermodynamic properties, which were determined through equilibrium simulations. All
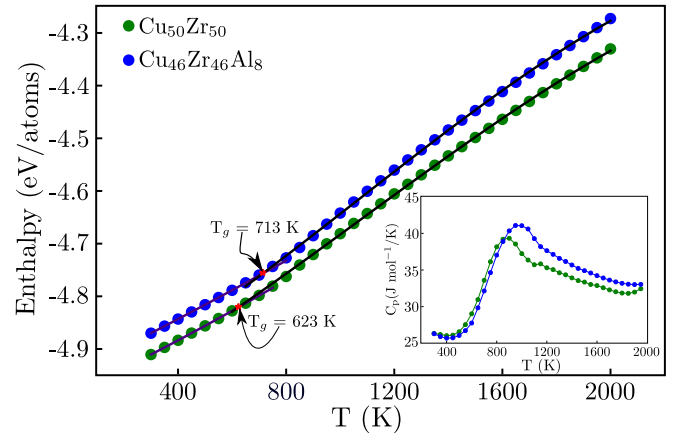

FIG. 1. Enthalpy per atom of binary $Cu_{50}Zr_{50}$ and ternary $Cu_{46}Zr_{46}Al_8$ alloys as a function of temperature extracted from MD equilibrium simulations. The error bars are of the size of the symbols. Two fitting functions were used to obtain the glass transition temperature (see text). The inset shows the isobaric heat capacity C_p behavior for the same alloys.

correlation functions were calculated in the canonical (NVT) ensemble.

We repeated the same procedure for two ternary alloys ($x = 49, 46$) and analyzed the behavior of the viscosity, self-diffusion coefficient, and vibrational density of states with the aluminum percentage increase.

B. Glass transition

As the quench was being carried out, we saved atomic configurations every 50 K in order to obtain thermodynamic information during the cooling process. These configurations were used as input in MD equilibrium simulations. After thermalization, thermodynamic properties were determined from MD equilibrium simulations comprising 10^6 time steps. The behavior of the enthalpy and isobaric heat capacity as a function of temperature for binary $Cu_{50}Zr_{50}$ and ternary $Cu_{46}Zr_{46}Al_8$ are presented in Fig. 1. The isobaric heat capacity C_p defined through the derivative of the enthalpy

$$C_p = \left(\frac{\partial H}{\partial T}\right)_p \tag{1}$$

was used to estimate the glass transition temperature T_g. For solid and liquid states, C_p is expressed by the equations

$$C_p = 3k_B + cT + dT^2 \tag{2}$$

and

$$C_p = 3k_B + aT^2 + \frac{b}{T^2}, \tag{3}$$

respectively. Equation (2) is the solid correction to the Dulong-Petit law and Eq. (3) is the Kubaschewski relation to describe the C_p of liquids [32]. In order to estimate the value of T_g, we integrate Eqs. (2) and (3) to obtain the enthalpy of the two states. The magenta line in Fig. 1 is obtained by fitting the results for the liquid state to the equation for the enthalpy of the liquid, in the interval of 1400–900 K, while the orange line is obtained by fitting the data for the solid state to the equation

TABLE I. Glass transition temperature T_g obtained in this work, from experiments, and from other computational studies for the three $Cu_xZr_xAl_{100-2x}$ alloys ($x = 50, 49, 46$).

Alloy	T_g (K)[a]	T_g (K)[b]
$Cu_{50}Zr_{50}$	623	664
$Cu_{49}Zr_{49}Al_2$	632	674
$Cu_{46}Zr_{46}Al_8$	713	701

[a]This work.
[b]Reference [15].

for the enthalpy of the solid, in the range of 500–300 K. The estimated values for T_g are approximately 623 K for the binary alloy and 713 K for the ternary $Cu_{46}Zr_{46}Al_8$, such values were obtained by intersecting the two fitting curves. These results agree with previous experimental and theoretical estimates for T_g of CuZr(Al) alloys [15,33]. A peak in C_p (inset Fig. 1) is also an evidence that glass transition occurs in that range of temperatures.

For the ternary $Cu_{49}Zr_{49}Al_2$ alloy, a similar procedure was employed to obtain $T_g \approx 632$ K; these results are not shown in detail to avoid repetition. In Table I the values of T_g we have determined for each alloy are compared with those obtained experimentally in Ref. [15].

C. Dynamic properties

In order to evidence the FSC, we studied three dynamical properties: diffusion coefficient, vibrational density of states, and shear viscosity of the $Cu_xZr_xAl_{100-2x}$ alloys.

First, the diffusion coefficient was computed using molecular dynamics simulations through the mean-squared displacement (MSD) of each atom

$$\langle r^2(t) \rangle = \frac{1}{N} \left\langle \sum_{l=1}^{N} |r_l(t) - r_l(0)|^2 \right\rangle, \qquad (4)$$

where $r_l(t)$ is the position vector of the lth particle at time t. For long times, the particles are in the diffusive regime, and the MSD is linearly dependent on time. Consequently, the diffusion can be calculated by the equation

$$D = \lim_{t \to \infty} \frac{1}{6t} \langle |r_i(t) - r_i(0)|^2 \rangle. \qquad (5)$$

Based on previous studies, an excess in the vibrational density of states (VDOS) of low frequencies with respect to the Debye model is an evidence of a non-Arrhenius to Arrhenius behavior crossover in supercooled liquids [34,35]. The VDOS is determined using the Fourier transform of the normalized velocity autocorrelation function

$$g(\omega) = \frac{1}{N} \sum_{l=1}^{N} \int_{-\infty}^{\infty} \frac{\langle \vec{v}_l(t) \cdot \vec{v}_l(0) \rangle}{\langle \vec{v}_l(0) \cdot \vec{v}_l(0) \rangle} e^{i\omega t} dt, \qquad (6)$$

where $\vec{v}_l$ is the velocity vector of the lth particle at time t. At last, the shear viscosity was calculated using a Green-Kubo relation [36,37]

$$\eta = \frac{\beta V}{N} \int_0^{\infty} \langle P_{\alpha\gamma}(0) P_{\alpha\gamma}(t) \rangle dt, \qquad (7)$$

where β is the reciprocal of the absolute temperature times the Boltzmann constant $(k_B T)^{-1}$, V is the volume of the system, and $P_{\alpha\gamma}$ is an off-diagonal component, P_{xy}, P_{xz}, and P_{yz}, of the stress tensor. Following Alfè et al. [38], two more components should be included to calculate the viscosity in Eq. (7):

$$\frac{1}{2}(P_{xx} - P_{yy}) \qquad \text{and} \qquad \frac{1}{2}(P_{yy} - P_{zz}),$$

hence, five components were computed in order to obtain the shear viscosity.

As we will show later, the crossover temperature T_{fs} is greater when the Al percentage is increased, and this fact allows us to explore the shear viscosity behavior in the ternary $Cu_{46}Zr_{46}Al_8$ for the values in which the FSC is evidenced. We were not able to observe the crossover from the shear viscosity results of binary $Cu_{50}Zr_{50}$ and ternary $Cu_{49}Zr_{49}Al_2$ because the off-diagonal stress tensor components do not completely decorrelate even when the sampling time reached 5 ns and larger simulation sampling times would exceed our MD capabilities (see Sec. III C).

III. RESULTS AND DISCUSSION

A. Diffusion coefficient

Figure 2 shows the inverse of the diffusion coefficient (ID) as a function of the inverse temperature for the three alloys, calculated using Eq. (5). We observe a change in the behavior of ID at temperatures near the glass transition for the three alloys. Moreover, this change is shifted toward higher temperatures when aluminum concentration increases. This is due to the properties of MGFLs that strongly depend on composition [14,18]. The modification in the ID behavior can be associated with the existence of FSC at a certain temperature T_{fs}, where the crossover takes place. In order to find T_{fs} for the alloys, we fitted the data for high temperatures to the Vogel-Fulcher-Tamman (VFT) equation [39–41]

$$D = D_0 \exp\left(-\frac{A}{T - T_0}\right), \qquad (8)$$

where A is a parameter that indicates by how much the diffusion diverges from the Arrhenius behavior when the temperature decreases, T_0 is the temperature at which the ID diverges, and the factor D_0 is the diffusion coefficient extrapolated to infinite temperature. Previous studies of CuZr(Al) alloys reveal a dynamical decoupling happening at a temperature $T_A \approx 1200$ K [24,26]. This decoupling is associated with the beginning of the dynamical heterogeneities. Above T_A, the liquid alloy presents a non-Arrhenius behavior, therefore, for our purposes we fitted our data to a VFT equation for temperatures below T_A, for each alloy.

The solid red lines in Fig. 2 are obtained by the fitting the data to a VFT equation. For low temperatures, close to T_g (red shaded region in Fig. 2), the values for ID are not well fitted by Eq. (8). In this region, it is more appropriate to fit to an Arrhenius equation as follows:

$$D = D_A \exp\left(-\frac{E_A}{k_B T}\right), \qquad (9)$$

where E_A is the constant activation energy characteristic of a strong liquid [3,6]. The dashed blue lines in Fig. 2 represent
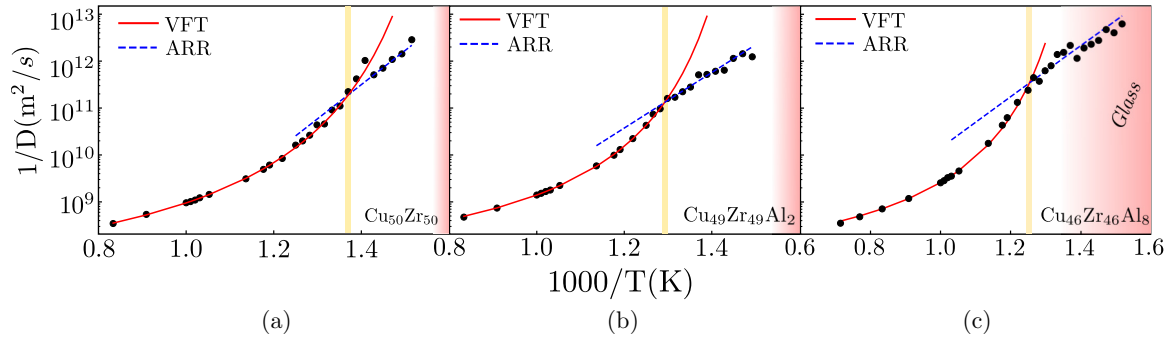
FIG. 2. Temperature dependence of the inverse diffusion coefficient of the three alloys: (a) $Cu_{50}Zr_{50}$, (b) $Cu_{49}Zr_{49}Al_2$, and (c) $Cu_{46}Zr_{46}Al_8$. The red line indicates the fitting to a VFT equation and blue dashed is an Arrhenius fit. Yellow shaded region marks the fragile-to-strong crossover.

the fit to an Arrhenius equation. At the crossover temperature T_{fs}, the contributions from the fragile and the strong regions to the whole dynamics are the same, i.e., the temperature at which the values for the diffusion coefficient calculated from Eqs. (8) and (9) are equal. For the binary $Cu_{50}Zr_{50}$ the FSC happens at 730 K. However, for the ternary alloys $Cu_{49}Zr_{49}Al_2$ and $Cu_{46}Zr_{46}Al_8$ the FSC occurs at 774 and 797 K, respectively, suggesting a relation between glass transition and FSC as is put forward by Mallamace *et al.* [42]. Table II shows the values for the fitting parameters and the crossover temperature of the three alloys.

The values we have obtained for T_{fs} are significantly lower than those previously reported for these alloys [15,18,23]. However, in a recent study, Sukhomlinov and Müser [43,44] obtained a value for T_{fs} similar to ours, performing molecular dynamics simulations in the $Cu_{29}Zr_{60.6}Al_{10.4}$ alloy. Since it is very difficult for the experiments to probe directly the molten alloy in the supercooled regime, the experimental estimates of the FSC temperature were determined from models to interpolate the experimental results for viscosity obtained at high temperatures (above the first crossover) and at low temperatures just above the glass transition [15]. We believe this is the main reason why the experimental FSC temperature estimates are significantly higher than ours. Regarding the computational studies of the FSC in these alloys [18,23], their estimates for the FSC temperature are based on indirect evidence of the FSC, instead of a direct observation of the change in behavior from non-Arrhenius to Arrhenius in either the diffusion coefficient or the shear viscosity. This difference in approach can explain the discrepancies between their results and our findings. Following the previous study in Ref. [44] about the finite-size effects in the FSC for CuZrAl-based metallic glass we explore the size effect in our calculations. In Fig. 3 is shown the behavior of the inverse coefficient

diffusion as a function the temperature of the ternary $Cu_{46}Zr_{46}Al_8$ using two supercells, the first one with $N = 4000$ atoms used in whole our work, and the second one with $N = 8000$ atoms to show that our results are not changed when the simulation cell increased. As Sukhomlinov and Müser pointed in their work, size effect decreases with N, this being the reason because for $T < T_{fs}$ the fluctuation in the inverse of diffusion coefficient is lesser when $N = 4000$ than $N = 8000$.

B. Vibrational density of states

Glasses present an excess of vibrational modes in the VDOS compared to Debye law [$g(\omega) \propto \omega^2$] at low temperatures [45]. This excess of modes appears as a peak in the reduced VDOS (rVDOS), defined as $g(\omega)/\omega^2$, known as boson peak (BP) [16,46,47]. The previous studies about the BP show that the excess in VDOS is more pronounced in strong liquids than in fragile liquids [48]. Therefore, we used as a criterion for the occurrence of the FSC a pronounced BP at low temperatures characteristic of strong liquids.

The rVDOS and VDOS for $Cu_{50}Zr_{50}$ obtained using Eq. (6) are depicted in Fig. 4. For temperatures above 1000 K the rVDOS decreases monotonically with increasing ω. Notwithstanding, the deviation from the Debye law appears at 750 K. However, as showed previously in the behavior of ID, the FSC does not occur for this temperature and the BP appears as a weak deviation from the Debye law. Moreover, a pronounced boson peak appears only at temperatures below 750 K at approximately 1.7 THz, evidencing a change in the behavior of the rVDOS, which could be associated with a FSC in the interval 750–700 K. Those results are consistent with the crossover temperature T_{fs} obtained from the prior calculation of ID for the same alloy.

TABLE II. Fitting parameters of the VFT and the Arrhenius equations, and fragile-to-strong temperature T_{fs} for the three CuZr(Al) alloys.

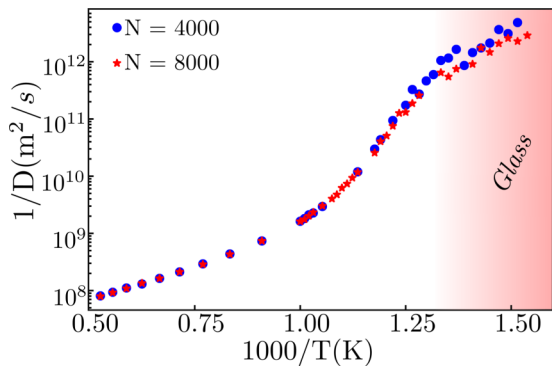| Alloy	D_0 (m^2/s)$\times 10^{-8}$	A	T_0 (K)	D_A (m^2/s)$\times 10^{-3}$	E_A (eV)	T_{fs} (K)[a]	T_{fs} (K)[b]
$Cu_{50}Zr_{50}$	2.36	1333.35	571	49.23	1.44	730	989
$Cu_{49}Zr_{49}Al_2$	1.98	1232.81	623	1.12	1.27	774	1047
$Cu_{46}Zr_{46}Al_8$	2.31	1272.53	650	417	1.11	797	1059

[a]This work.
[b]Reference [15].

FIG. 3. Inverse of the diffusion coefficient as a function of temperature for the ternary $Cu_{46}Zr_{46}Al_8$ metallic alloy for simulation cells $N = 4000$ atoms and $N = 8000$ atoms. From the graph one can see that T_{fs} remains unaltered.

In Fig. 5 we show the rVDOS and the VDOS for the ternary alloy $Cu_{46}Zr_{46}Al_8$. For temperatures above 1000 K the liquid does not present any excess modes in the rVDOS, similarly to the case of the binary alloy $Cu_{50}Zr_{50}$. At 800 K we observe a pronounced boson peak. Additionally, for 750 and 700 K we see that the peaks are frequency shifted in comparison to the binary alloy, happening at approximately 6.8 and 6.2 THz, respectively. In contrast with the binary alloy a pronounced boson peak appears at 800 K and approximately 7.5 THz, evidencing that the FSC is shifted for higher temperatures when the Al percentage is increased.

We do not show a similar set of curves for $Cu_{49}Zr_{49}Al_2$ because the behavior is analogous to the $Cu_{50}Zr_{50}$ alloy. Nonetheless, the results are included in the Supplemental Material [49]. In order to provide an additional evidence of the FSC, we analyze the shear viscosity of these CuZr(Al) alloys in the next subsection.

C. Shear viscosity

In order to calculate the shear viscosity using Eq. (7), the average of the autocorrelation function (C_{pp}) of the five components of the tension tensor $\langle P_{\alpha\gamma}(t)P_{\alpha\gamma}(0)\rangle$ must be calculated and integrated over all the history of the system. Figure 6 depicts the behavior C_{pp} as a function of time for the
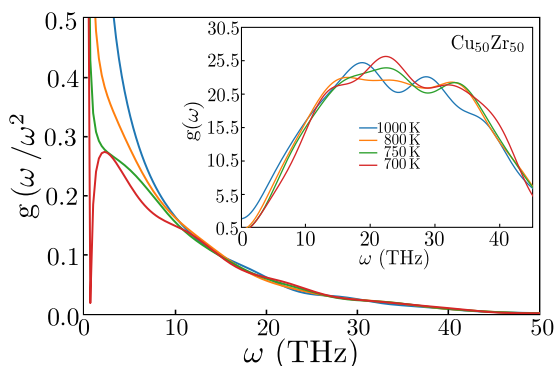

FIG. 4. rVDOS and VDOS (inset) of the $Cu_{50}Zr_{50}$ alloy as a function of angular frequency for different temperatures. A pronounced boson peak appears for temperatures below 750 K, at approximately 1.2 THz.
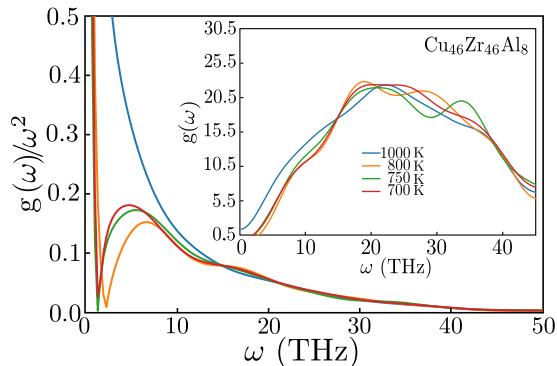

FIG. 5. rVDOS and VDOS (inset) of the $Cu_{46}Zr_{46}Al_8$ alloy as a function of angular frequency for different temperatures. The boson peak that appears below 1000 K shifts toward lower frequencies as the temperature decreases.

ternary $Cu_{46}Zr_{46}Al_8$ alloy. For temperatures below 1300 K, C_{pp} shows a dramatic slowing down of the relaxation dynamics, this is due to the onset of dynamical heterogeneity that occurs at the characteristic temperature T_A, which is reported to lie in the interval 1000–1300 K for the CuZr(Al) metallic alloys [24,26]. For temperatures lower than 790 K, the C_{pp} does not decorrelate for $t = 5$ ns, presenting a prohibitive computational cost in order to calculate reliable values of viscosity for these temperatures. In the case of binary $Cu_{50}Zr_{50}$
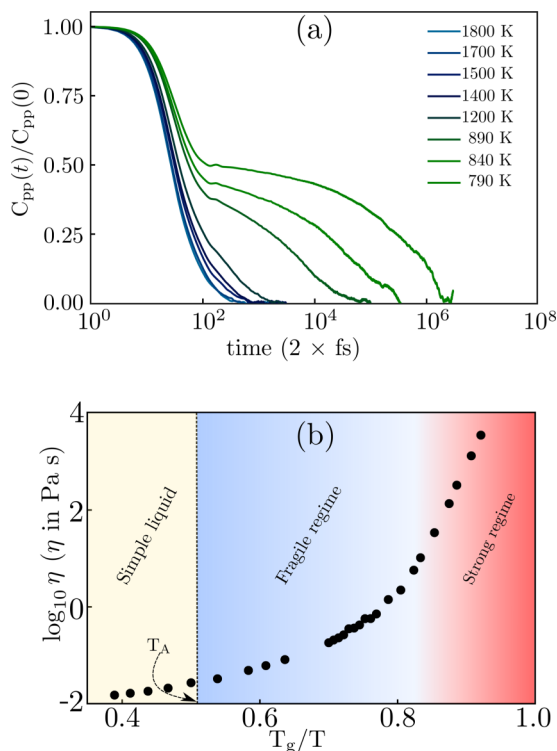

FIG. 6. (a) Averaged autocorrelation function C_{pp} as a function of time and (b) logarithm of the shear viscosity as a function of the reduced temperature T_g/T for $Cu_{46}Zr_{46}Al_8$. C_{pp} shows a slowing down in the relaxation dynamics for temperatures below 1200 K. Three regimes are well defined in the viscosity behavior, showing the two typical crossovers in supercooled liquids.
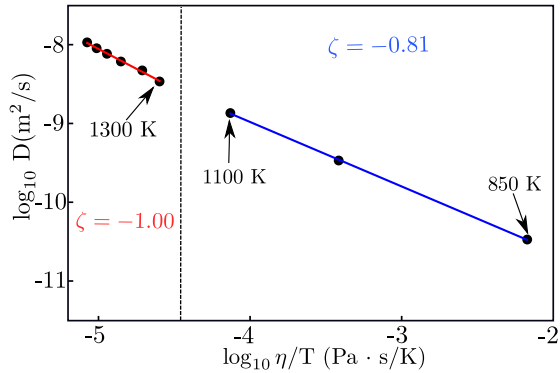
FIG. 7. The SE relation for $Cu_{46}Zr_{46}Al_8$. For high temperatures, in the interval 1800–1300 K, the slope is $\zeta = -1$. However, for temperatures below $T_A = 1200$ K, the SE relation deviates from the ideal to a fractional form with $\zeta = -0.81$.

and ternary $Cu_{49}Zr_{49}Al_2$, it was not possible calculate C_{pp} for temperatures at which the FSC could be observed. The reason why that happens was explained by Cheng *et al.* [28] through the differences between binary and ternary alloys regarding the development of icosahedral clusters as their respective liquids are quenched. By comparing the α-relaxation time, which scales with the viscosity, for CuZr and CuZrAl, Cheng *et al.* concluded that τ_α of the ternary alloy is at least one order of magnitude higher than that of the binary alloy. That is the reason why in our case we were only able to observe the FSC for the ternary alloy $Cu_{46}Zr_{46}Al_8$ since the T_{fs} is shifted toward higher temperatures when Al percentage increases.

The behavior of the logarithm of the shear viscosity as a function of reduced temperature (T/T_g) is displayed in Fig. 6. Three regimes can be identified during the cooling process. At first, for high temperatures, the alloy presents an Arrhenius behavior when the temperature decreases until approximately 1200 K. This first crossover from Arrhenius to non-Arrhenius behavior is associated with the beginning of the dynamical heterogeneity at specific temperature T_A, i.e., the mobilities differ by orders of magnitude in regions few nanometers away. For the case of MGFLs based in CuZrAl, previous studies have shown that this value occurs for a temperature close to 1300 K [24,50]. Our calculations lead to a value for T_A of 1200 K, which is in good agreement with previous studies of these alloys [26]. For temperatures below T_A, the shear viscosity develops a non-Arrhenius behavior, which is represented in Fig. 6 by the blue region. The FSC occurs at the reduced temperature of 0.85 (≈ 840 K); again, this value for T_{fs} agrees quite well with those obtained through ID and rVDOS for this alloy. Our estimates for T_{fs} are significantly lower than those reported in almost all previous studies of these MGFLs [15,23].

Finally, in Fig. 7 we show the behavior of the logarithm of the diffusion coefficient as a function of corresponding logarithm of the viscosity, both computed at the same temperature, in order to check the Stokes-Einstein relation (SE) for $Cu_{46}Zr_{46}Al_8$ alloy. This relation establishes a connection between the diffusion coefficient and the shear viscosity through the relation $D \sim (\eta/T)^\zeta$, which is strictly valid only for $\zeta = -1$. However, for the ternary alloy this behavior departs

from the ideal one to a fractional relation for temperatures below T_A, with $\zeta = -0.81$. This violation of SE relation from $\zeta = -1.00$ to $\zeta = -0.81$ is associated with a crossover from Arrhenius behavior to non-Arrhenius when the alloys are cooled below T_A.

IV. CONCLUSIONS

Three dynamic properties showing the existence of a FSC in $Cu_xZr_xAl_{100-2x}$ with $x = 50, 49, 46$ were calculated through MD simulations. Two dynamical crossovers are evidenced during the cooling process. The first crossover is associated with the dynamical heterogeneities, and marks onset of the non-Arrhenius behavior before the liquid enters in the supercooled regime. By investigating the ID for temperatures below T_A for $Cu_{50}Zr_{50}$, $Cu_{49}Zr_{49}Al_2$, and $Cu_{46}Zr_{46}Al_8$ we observed two regimes well defined. The first regime exhibits a non-Arrhenius behavior fitted to a VFT equation and a second regime, which displays an Arrhenius behavior. From that we are able to estimate the temperature at which the crossover occurs. Our findings for the FSC temperature are significantly lower than nearly all previous estimates from experiments and computer simulations, notwithstanding, we obtained a value for T_{fs} in agreement with recent studies using MD with the same interatomic potential [43,44]. The reason for these discrepancies with past works possibly stems from the fact that in these studies the FSC temperature determination relies on indirect evidence of the crossover, instead of the direct observation of the change in behavior from non-Arrhenius to Arrhenius in either the diffusion coefficient or the shear viscosity.

The rVDOS reveals a pronounced BP at low temperatures, which can be considered as an evidence of FSC. In the case of the binary $Cu_{50}Zr_{50}$, a pronounced BP is only observed for temperatures below 750 K. Notwithstanding the appearing of BP coincides with the value T_{fs} obtained through of the ID.

We also investigated the breakdown of the SE relation for the $Cu_{46}Zr_{46}Al_8$ alloy that occurs below T_A. Our results agree with previous computational studies of similar alloys [18,24]. Finally, we explain the origin of FSC and how the Al presence increases the FSC temperature T_{fs} within the framework of the potential energy landscape (PEL) theory [51,52], the PEL of a liquid at high temperatures is composed by basins separated by energy barriers that are uniform throughout the configuration space available for the system. The transition between basis, in this case, corresponds to localized rearrangement of atoms. This process is usually called β. The uniformity of the energy barriers between basins explains the Arrhenius behavior exhibited by diffusion and viscosity of the liquid at high temperatures. As the liquid is further cooled down to the supercooled regime, the behavior of these properties changes to non-Arrhenius, as dynamical heterogeneities set in. This can be understood as consequence of the change in the topography of the PEL. In this regime, the PEL is formed by metabasins (or craters), which are themselves composed by basins separated by energy barriers that are uniform throughout the metabasin. The energy barriers between metabasins are larger than those separating the basins within the metabasins. In this case, two types of processes can happen: transitions between basins, β processes,

and transitions between metabasins, usually named α. The multiple activation energies of these processes can explain the non-Arrhenius behavior of the liquid. According to the PEL theory, the α processes require the concerted rearrangement of a large number of atoms, which gives a delocalized character to these processes. As the liquid is further cooled, there will be a temperature below which the system will be unable to overcome the energy barriers between metabasins and the α processes will cease to occur. Thus, below that temperature diffusion and viscosity will again display an Arrhenius behavior, since only β processes will occur. In other words, this is the temperature at which the fragile-to-strong crossover takes place (T_{fs}). Therefore, the larger the energy barriers between metabasins, the higher T_{fs} will be. Since the α process requires the rearrangement of many atoms, our results suggest that addition of a small amount of Al to the binary alloy will increase the energy required for the α transition to take place, thus providing an insight why the addition of small amounts of Al can increase significantly T_{fs}.

ACKNOWLEDGMENTS

[1] W. Klement, R. H. Willens, and P. Duwez, Nature (London) **187**, 869 (1960).

[2] P. W. Anderson, Science **267**, 1615 (1995).

[3] P. G. Debenedetti and F. H. Stillinger, Nature (London) **410**, 259 (2001).

[4] G. G. Naumis, Phys. Rev. B **73**, 172202 (2006).

[5] G. G. Naumis, J. Non-Cryst. Solids **352**, 4865 (2006).

[6] C. A. Angell, J. Non-Cryst. Solids **131–133**, 13 (1991).

[7] K. Ito, C. T. Moynihan, and C. A. Angell, Nature (London) **398**, 492 (1999).

[8] S.-H. Chen, F. Mallamace, C.-Y. Mou, M. Broccio, C. Corsaro, A. Faraone, and L. Liu, Proc. Natl. Acad. Sci. USA **103**, 12974 (2006).

[9] I. Saika-Voivod, P. H. Poole, and F. Sciortino, Nature (London) **412**, 514 (2001).

[10] I. Saika-Voivod, F. Sciortino, and P. H. Poole, Phys. Rev. E **69**, 041503 (2004).

[11] M. Hemmati, C. T. Moynihan, and C. A. Angell, J. Chem. Phys. **115**, 6663 (2001).

[12] M. C. Wilding, P. F. McMillan, and A. Navrotsky, Physica A (Amsterdam) **314**, 379 (2002).

[13] J. Wiedersich, A. Kudlik, J. Gottwald, G. Benini,, I. Roggatz, and E. Rössler, J. Phys. Chem. B **101** 5800 (1997).

[14] C. Zhang, L. Hu, Y. Yue, and J. C. Mauro, J. Chem. Phys. **133**, 014508 (2010).

[15] C. Zhou, L. Hu, Q. Sun, H. Zheng, C. Zhang, and Y. Yue, J. Chem. Phys. **142**, 064508 (2015).

[16] K. Trachenko and V. V. Brazhkin, J. Phys.: Condens. Matter **21**, 425104 (2009).

[17] S.-H. Chong, S.-H. Chen, and F. Mallamace, J. Phys.: Condens. Matter **21**, 504101 (2009).

[18] Y. Zhang, N. Mattern, and J. Eckert, J. Appl. Phys. **110**, 093506 (2011).

[19] B. Bochtler, O. Gross, and R. Busch, Appl. Phys. Lett. **111**, 261902 (2017).

[20] J. C. Phillips, Phys. Rev. B **73**, 104206 (2006).

[21] J. Langer, Phys. Today **60**(2), 8 (2007).

[22] Y. Zhang, N. Mattern, and J. Eckert, J. Alloys Compd. **514**, 141 (2012).

[23] K. N. Lad, N. Jakse, and A. Pasturel, J. Chem. Phys. **136**, 104509 (2012).

[24] F. Puosi, N. Jakse, and A. Pasturel, J. Phys.: Condens. Matter **30**, 145701 (2018).

[25] F. Li, H. Zhang, X. Liu, Y. Dong, C. Yu, and Z. Lu, J. Appl. Phys. **123**, 055101 (2018).

[26] A. Jaiswal, T. Egami, and Y. Zhang, Phys. Rev. B **91**, 134204 (2015).

[27] A. Foroughi, R. Tavakoli, and H. Aashuri, J. Non-Cryst. Solids **432**, 334 (2016).

[28] Y. Q. Cheng, E. Ma, and H. W. Sheng, Appl. Phys. Lett. **93**, 111913 (2008).

[29] Y. Q. Cheng, E. Ma, and H. W. Sheng, Phys. Rev. Lett. **102**, 245501 (2009).

[30] S. Plimpton, J. Comput. Phys. **117**, 1 (1995).

[31] M. S. Daw and M. I. Baskes, Phys. Rev. B **29**, 6443 (1984).

[32] O. Kubaschewski, C. B. Alcock, and P. J. Spencer, in *Materials Thermochemistry* (Pergamon Press, Oxford, 1993), p. 363.

[33] Y. Zhang, N. Mattern, and J. Eckert, J. Appl. Phys. **111**, 053520 (2012).

[34] S. Cajahuaringa, M. De Koning, and A. Antonelli, J. Chem. Phys. **139**, 224504 (2013).

[35] N. Jakse and A. Pasturel, Appl. Phys. Lett. **93**, 113104 (2008).

[36] J.-P. Hansen and I. R. I. R. McDonald, in *Theory of Simple Liquids: With Applications to Soft Matter* (Academic Press, Oxford, 2013), p. 619.

[37] M. P. Allen and D. J. Tildesley, *Computer Simulation of Liquids* (Oxford University Press, Oxford, 1987).

[38] D. Alfè and M. J. Gillan, Phys. Rev. Lett. **81**, 5161 (1998).

[39] D. H. Vogel, Phys. Z. **22**, 645 (1921).

[40] G. S. Fulcher, J. Am. Ceram. Soc. **8**, 339 (1925).

[41] G. Tammann and W. Hesse, Z. Anorg. Allg. Chem. **156**, 245 (1926).

[42] F. Mallamace, C. Branca, C. Corsaro, N. Leone, J. Spooren, S.-H. Chen, and H. E. Stanley, Proc. Natl. Acad. Sci. USA **107**, 22457 (2010).

[43] S. V. Sukhomlinov and M. H. Müser, Phys. Rev. Mater. **2**, 115604 (2018).

[44] S. V. Sukhomlinov and M. H. Müser, Comput. Mater. Sci. **156**, 129 (2019).

[45] T. S. Grigera, V. Martín-Mayor, G. Parisi, and P. Verrocchio, Nature (London) **422**, 289 (2003).

[46] A. Monaco, A. I. Chumakov, G. Monaco, W. A. Crichton, A. Meyer, L. Comez, D. Fioretto, J. Korecki, and R. Rüffer, Phys. Rev. Lett. **97**, 135501 (2006).

[47] A. I. Chumakov, I. Sergueev, U. Van Bürck, W. Schirmacher, T. Asthalter, R. Rüffer, O. Leupold, and W. Petry, Phys. Rev. Lett. **92**, 245508 (2004).

[48] A. P. Sokolov, E. Rössler, A. Kisliuk, and D. Quitmann, Phys. Rev. Lett. **71**, 2062 (1993).

[49] See Supplemental Material at http://link.aps.org/supplemental/10.1103/PhysRevMaterials.3.085601 for behavior of the auto-correlation velocity function and reduced vibrational density of states for the $Cu_{49}Zr_{49}Al_2$ alloy.

[50] H. Zhang, C. Zhong, J. F. Douglas, X. Wang, Q. Cao, D. Zhang, and J.-Z. Jiang, J. Chem. Phys. **142**, 144503 (2015).

[51] F. H. Stillinger, Science **267**, 1935 (1995).

[52] F. Stillinger, *Energy Landscapes, Inherent Structures, and Condensed Matter Phenomena* (Princeton University Press, Princeton, NJ, 2015).